Proceedings of the 2019 Design of Medical Devices Conference
DMD2019
April 15, 16-18, 2019, Minneapolis, MN, USA

DMD2019-3313

TUNEABLE RESONANCE ACTUATORS FOR MAGNETIC RESONANCE ELASTOGRAPHY

Waiman Meinhold
Georgia Institute of Technology
Atlanta, Georgia, USA
wmeinhold@gatech.edu

Efe Ozkaya
Stevens Institute of Technology
Hoboken, New Jersey, USA

Jun Ueda
Georgia Institute of Technology
Atlanta, Georgia, USA

Mehmet Kurt
Stevens Institute of Technology
Hoboken, New Jersey, USA

ABSTRACT

Palpation, or physical manipulation of tissue to assess mechanical properties is one of the most prevalent and valuable clinical evaluations. Because physical interaction is needed, historically palpation has been limited to easily accessible surface level tissues. Magnetic resonance elastography (MRE) combines non-invasive Magnetic Resonance Imaging(MRI) with mechanically induced shear waves, producing the ability to map elasticity of soft tissues in vivo. Actuator design has been a limiting factor in MRE advancements. In this study, a mechanical resonator with adjustable resonant frequency was designed to be used in MRE applications. The designed piezoelectric actuator was fully MRI compatible, and capable of dynamically adjusting its resonant frequency. The purpose was to keep the displacement amplitude sufficiently large over a wide actuation frequency range. The outer stage of the amplifier contained movable side masses for tuning resonance frequency.

Keywords: magnetic resonance elastography

1 INTRODUCTION

Palpation of tissue to assess mechanical properties is one of the oldest medical techniques, and still in widespread use today. For a large number of tissues, shear modulus is a clinically important mechanical property. Currently, this parameter is acquired by a non-invasive *in vivo* imaging technique, Magnetic Resonance Elastography (MRE), a phased-contrast based MRI technique [1,2]. MRE involves the generation of shear waves along the tissue of interest by an actuator and capturing of the displacement field, then calculation of elastograms through an inversion algorithm. The shear displacements are imaged via Magnetic Resonance Imaging (MRI). The necessity of MRI compatibility significantly restricts available actuation modalities for this technique.

1.1 MRE Actuator Design

MRE actuator design has been a critical impediment to progression of the technique to small and stiff tissues. Mechanical characterization of deep-set smaller soft tissues has been limited due to wave attenuation and wave lengths. Previous efforts have attempted to improve actuation technology, but have often involved force transmission methods that are inherently non-compact and frequency limited [3,4]. Existing actuation methods include primarily remote electromechanical drivers and piezoelectric actuators, with limited work in pneumatic actuation.

Electromechanical drivers require an alternating current to be passed through a coil that generates oscillatory motion. An extension is mechanically coupled with the moving coil through which the excitation is transmitted to the patient. Loudspeakers are commonly used as the actuation method, with pneumatic or rigid coupling to the patient. Some of the first MRE work involved a vibration motor rigidly coupled to a plate in the scanner bore by a long plexiglass rod [5]. The only actuation modality currently FDA approved is pneumatic coupling of a loudspeaker type driver to the subject [6]. This type of coupling solves the orientation and space constraints associated with rigid transmission rods, but is frequency limited because of the use of air as a transmission media. Nevertheless, pneumatic transmission systems are used clinically for MRE of the liver, as well as brain MRE in research settings [7].

Mariappan et al. demonstrated the concept of wave optimization in which phased-array drivers were used simultaneously. At certain regions of interest, constructive wave

interference was arranged by optimization of timing of individual drive shafts [1]. Shrinking of the form factor of actuators should aid in future resolution enhancement methods by reducing placement constraints and increasing accuracy.

In addition to the pneumatic transmission methods detailed above, pneumatic actuation methods have also been studied for MRE. Although work in this area is much more limited, two groups have presented designs utilizing unbalanced rotational mechanisms as MRE actuators [8, 9]. One design used a rotary ball actuator, in which air drives a polymer ball around a circular path [8], while the other used a 3D printed turbine [9]. Fundamentally, both designs include a rotary actuator driven by flowing air, resulting in an actuation frequency proportional to the driven rotation speed. This gives a truly pneumatic actuator with higher achievable frequencies than pneumatic transmission methods, with a reported maximum of 240 Hz, still far too low for high resolution MRE of small tissues. It is possible that actuation frequency could be increased with a higher supply pressure, but with such high pressures and a rotational speed of 60,000 RPM for 1 kHz actuation, safety will be difficult to ensure. In

Piezoelectric actuators have been explored as potential solutions to the transmission and frequency problems detailed in the preceding sections. Piezoelectric materials are MRI compatible, and MR safe actuators can be made from these materials, and safely placed in close proximity to patients with minimal image distortion [10]. Lever systems for displacement amplification combined with a piezo actuator [10], a piezoelectric bending element with needle positioned parallel to the plane surface [11], piezoelectric ceramic connected to a phantom surface with a slim plexiglass plate [12], and a piezoceramic actuator with a compliant mechanical amplifier [13] are few actuator setups that have been used for MRE measurements. The main problem with piezoelectric actuators is their effective displacement gets smaller as actuation frequency is increased. This is often mitigated by integration with displacement amplification structures.

The viscoelasticity of soft tissues means that they exhibit frequency dependent behavior. This necessitates the use of multiple excitation frequencies during MRE for better mechanical characterization. While piezoelectric actuators for MRE have been proposed, they have fixed resonances, and thus are relatively bandwith limited [13]. Sufficient displacement is only achievable over a small frequency range.

In this study, we propose and develop an MRI compatible resonator whose resonance frequency was tunable. This allows a much larger range of MRE frequencies than previously developed actuators, allowing a larger number of tissues to be imaged.

2 METHODS

A resonance shifting MRE actuator was designed, built, characterized in simulation and evaluated for MRI compatibility.

2.1 Frequency Tuning Design

Although piezoelectric actuators are capable of extremely accurate motion and high forces, they suffer from extremely small strains. The standard method to combat this is mechanical strain amplification. Detailed below is the design of a mechanical resonator with a tuneable resonant frequency. The resonant frequency is adjusted by sliding the two masses on either side, changing both the inertial and stiffness characteristics of the actuator. The proposed design is shown in Figure 1.

The resonator design was chosen to provide the amplified motion perpendicular to the actuation of the ceramic, as the dimension can be increased to increase the input strain. The length of the actuator frame was constrained by the bore diameter of the available small animal scanner for testing. The height was chosen to fit a commercially available actuator, and the thickness matched to the available 655 bronze plate.

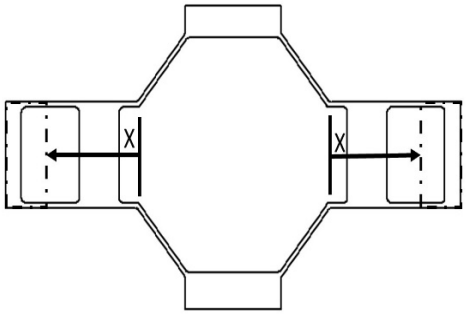

FIGURE 1: TUNABLE RESONANT ACTUATOR FRAME WITH SLIDING SIDE MASS

From this point, the wall thickness of the actuator was adjusted to capture the 650-1100 Hz range expected for the high frequency MRE application. FEM Modal analysis was done on a preliminary model of the resonator to determine the thickness that would produce a resonant frequency range overlapping with the expected high frequency MRE range. The results are shown in Figure 2. From this, a thickness of 0.5 mm is used, as this gives a 680-1117 Hz resonance range.

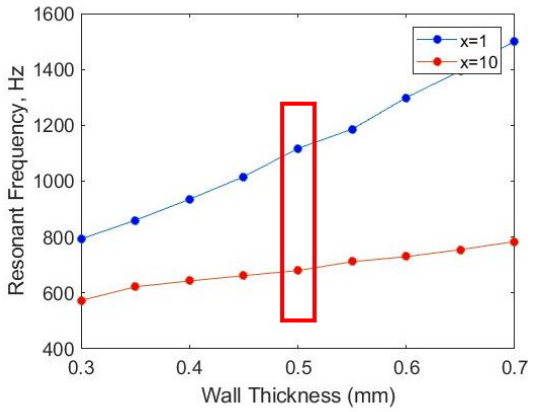

FIGURE 2: EFFECT OF WALL THICKNESS ON TUNING RANGE; RED BOX SHOWS THE CHOSEN VALUE OF 0.5 MM.

An implementation of the resonance frequency shifting design is shown in Figure 3. The sliding masses are embodied by the use of two linear piezoelectric actuators. In this case, scaled versions of Piezo LEGS 6N actuators are shown (PiezoMotor, Uppsala, Sweden), however any MRI compatible linear actuator is viable, as long as it fits within the geometric constraints. Tuning is not expected to take place at high frequencies, so even hydraulic or other slower actuators could be used. Linear piezoelectric actuators were chosen here because of the location precision required.

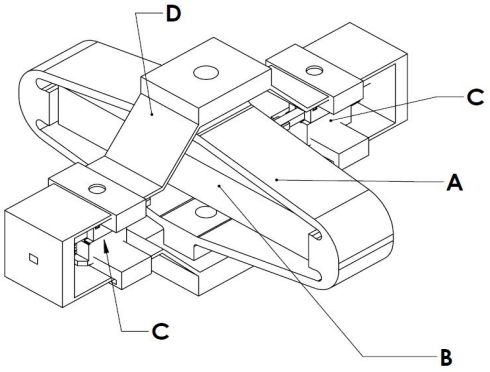

FIGURE 3: RESONANCE TUNING MECHANISM; A) APA 150M FRAME, B)PIEZOCERAMIC STACK, C)LINEAR PIEZOELECTRIC ACTUATOR, D) 655 BRONZE FRAME.

2.2 Fabrication

For evaluation purposes, 3 fixed frames were machined from 655 silicon bronze as shown in Figure 4. Chosen mass locations were 1, 5 and, 10 mm. The lower, middle, and upper ends of the positioning range. This is analogous to the adjustment of mass locations by linear piezoelectric actuator or another method. This resonant frame was combined with a commercially available amplified piezoelectric actuator (APA 150M, CEDRAT).

In practice, the resonant frame concept is not restricted to a particular choice of piezoelectric stack or amplifier. The fabricated frames and resonant actuator are shown in Figure 4.

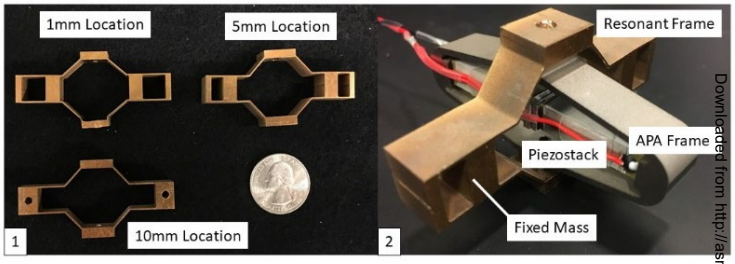

FIGURE 4: 1) FABRICATED BRONZE RESONANT FRAMES 2)APA 150M ACTUATOR AND RESONANT FRAME.

2.3 Finite Element Analysis

In addition to the parameter search detailed in section 2.1 and shown in Figure 2, a modal analysis was performed to validate the resonant frequency tuning concept (ANSYS 19.1., Ansys, Canonsburg, PA) The first 4 modes of each fabricated frame and APA actuator were compared. To confirm that the piezo actuation does not excite the lowest two modes, a harmonic analysis was completed. The piezoceramic stack shown in Figures 3 and 4 was replaced with a set pressure on the contact faces of the APA actuator. This confirmed that the 3rd resonant mode was excited during actuation, providing motion along the desired axis.

2.4 MRI Compatibility Assessment

A silicone rubber phantom was cast from DS30 and DS10 silicone rubber (Smooth-On Corp. Indiana). The stiffer outer ring was poured first, with DS 30, and then the softer inner region was poured from DS 10. The area and relative area of the two regions, as well as the thickness were approximately matched to the human intervertebral disc[14], a potential tissue for high frequency MRE imaging. The mold and 2 step casting process are shown in Figure 5.

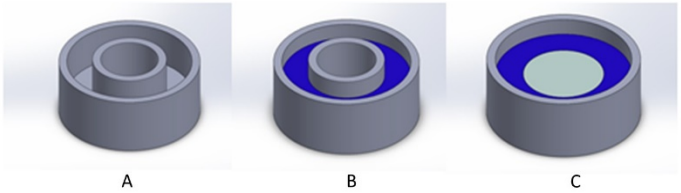

FIGURE 5: SILICONE PHANTOM FABRICATION PROCESS; A) ABS PLASTIC MOLD, B) OUTER DS10 SILICONE CASTED SILICONE, C) CENTRAL REGION POURED INTO CURED PHANTOM

The MRI safety and compatibility of the actuator was evaluated by imaging in a 7T scanner. The passive actuator was placed 10cm from a silicone rubber phantom, with a rigid polycarbonate connecting rod between the two. This stage is shown in Figure 6. Imaging was performed in the Mount Sinai TMII Imaging core facility, Mount Sinai, NY.

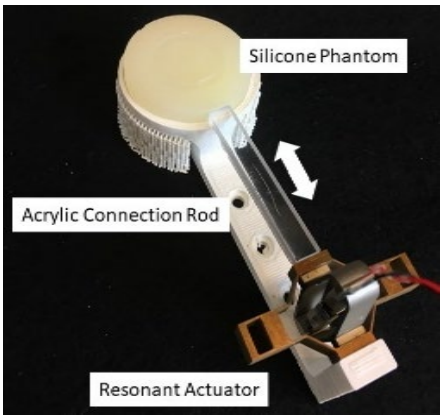

FIGURE 6: MRI EVALUATION STAGE

3 RESULTS

Figures 7-10 show the results of the modal analysis detailed in section 2.3. Figure 7 shows the results for the first mass location, at the lower end of the range. Figure 8 shows results for the x=5mm mass location, roughly in the middle of the range, and figure 9 shows results for the mass location at the upper end of the range. Figures 7 and 9 represent the upper and lower bounds for the resonant frequency range of the actuator.

Figures 10A-C show the isometric views of the 3rd mode for each of the mass locations. A harmonic study confirmed that this is the dominant mode during actuation by the APA actuator's piezostack. Figure 10D shows the resonant frequency for each of the 3 locations.

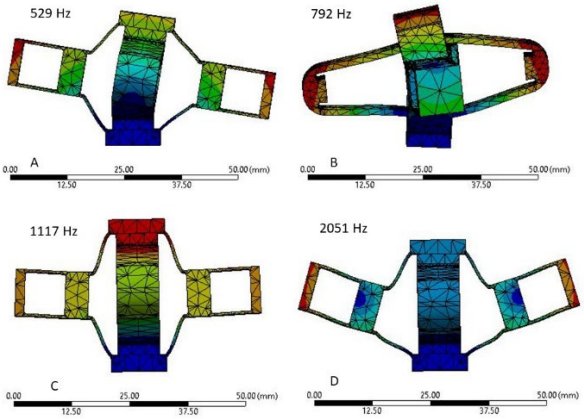

FIGURE 7: MODE SHAPES FOR MASS LOCATION OF 1MM; A) FIRST MODE B) SECOND MODE C)THIRD MODE D)FOURTH MODE.

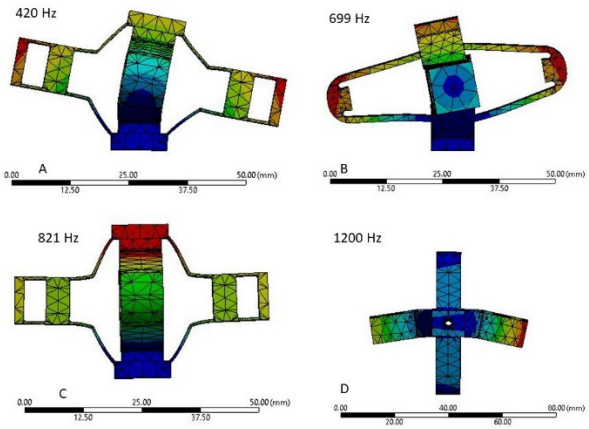

FIGURE 8: MODE SHAPES FOR MASS LOCATION OF 5MM; A) FIRST MODE B) SECOND MODE C)THIRD MODE D)FOURTH MODE.

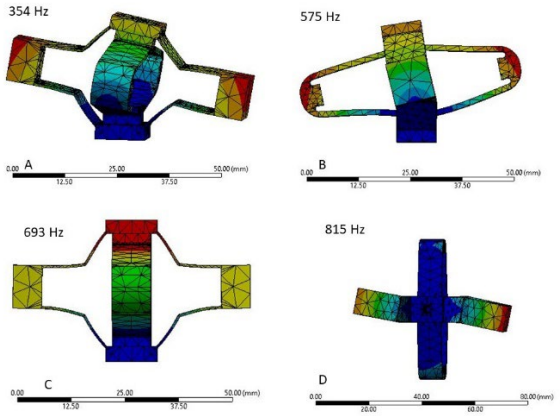

FIGURE 9: MODE SHAPES FOR MASS LOCATION OF 10MM; A) FIRST MODE B) SECOND MODE C)THIRD MODE D)FOURTH MODE.

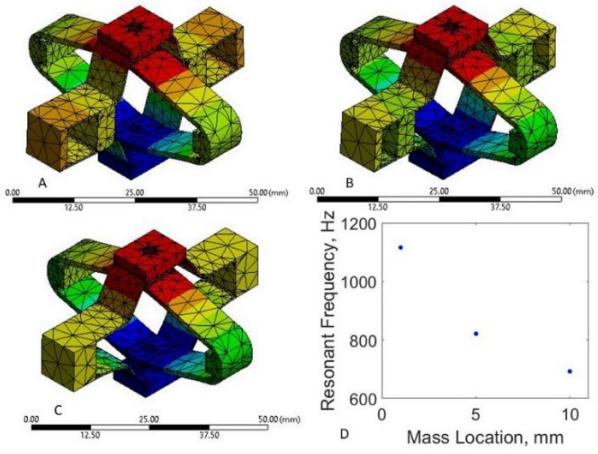

FIGURE 10: 3rd RESONANT MODE DISPLACMENT FOR EACH OF THE 3 FABRICATED FRAMES; A)1MM LOCATION B) 5MM LOCATION C)10MM LOCATION D)FREQUENCY-LOCATION PLOT.

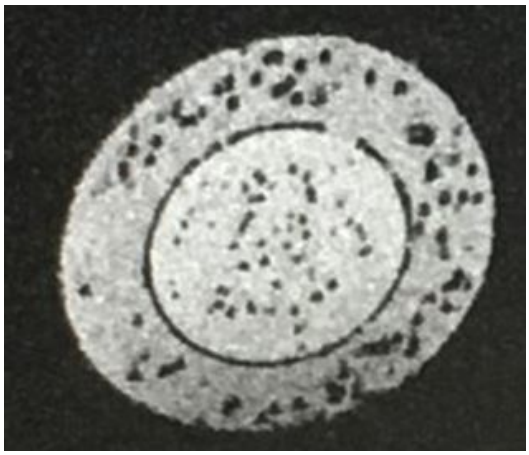

FIGURE 11: MAGNITUDE IMAGE OF THE PHANTOM LOCATED 10 CM FROM PASSIVE ACTUATOR

4 CONCLUSION

The results highlighted in Figure 7-10 demonstrate the validity of the proposed frequency tuning mechanism. Over a small 10 mm adjustment range, a 479 Hz resonance range was observed. Because the change in resonance is continuous with the position of the mass, the entirety of this range should be usable for MRE imaging. Changes in the geometry, materials, and piezo actuator will change this range, and work to optimize these parameters is ongoing. In addition, because the tunable resonator is similar in geometry to the typical mechanical amplifier, "stacking" or nesting of these structures should provide larger amplification ratios and an even larger frequency range.

Figure 11 demonstrates the MRI compatibility of the fabricated actuator assembly. The dark regions noted in the silicone are caused by air bubbles in the phantom, and the ring between the two materials is likely caused because of the boundary between the two different densities. The lack of interference from the actuator shows that the passive actuator does not noticeably impact image quality. Active tests should also be performed to ensure that the small current driving the actuator also has a negligible effect on image quality.

ACKNOWLEDGEMENTS

We thank Lazar Fleysher for help with MRI imaging. This work was partially supported by National Science Foundation under grant numbers 1545287 and 1317718, and Georgia Institute of Technology under the FY 18 GT FIRE and IRIM FY19 seed grant programs. Any opinions, findings, and conclusions or recommendations expressed in this material are those of the author(s) and do not necessarily reflect the views of the National Science Foundation.

REFERENCES

[1] Mariappan, Y. K., Rossman, P. J., Glaser, K. J., Manduca, A., and Ehman, R. L., 2009. "Magnetic resonance elastography with a phased-array acoustic driver system". Magnetic Resonance in Medicine, 61(3), Mar., pp. 678– 685.

[2] Low, G., 2016. "General review of magnetic resonance elastography". World Journal of Radiology, 8(1), p. 59.

[3] Uffmann, K., and Ladd, M., 2008. "Actuation Systems for MR Elastography". IEEE Engineering in Medicine and Biology Magazine, 27(3), May, pp. 28–34.

[4] Tse, Z. T. H., Chan, Y. J., Janssen, H., Hamed, A., Young, I., and Lamperth, M., 2011. "Piezoelectric actuator design for MR elastography: implementation and vibration issues". The International Journal of Medical Robotics and Computer Assisted Surgery, 7(3), Sept., pp. 353–360.

[5] Lewa, C. J., Roth, M., Nicol, L., Franconi, J.-M., and de Certaines, J. D., 2000. "A new fast and unsynchronized method for MRI of viscoelastic properties of soft tissues". Journal of Magnetic Resonance Imaging, 12(5), Nov., pp. 784–789.

[6] Resoundant. 2018. *Magnetic Resonance Elastography*. [online] Available at: https://docs.wixstatic.com/ugd/bd5a47_b8336bb232454af5905c54fd90b2eecc.pdf [Accessed 31 Oct. 2018].

[7] Johnson, C. L., and Telzer, E. H., 2017. "Magnetic resonance elastography for examining developmental changes in the mechanical properties of the brain". Developmental Cognitive Neuroscience, Sept

[8] Numano, T., Kawabata, Y., Mizuhara, K., Washio, T., Nitta, N., and Homma, K., 2013. "Magnetic resonance elastography using an air ballactuator". Magnetic Resonance Imaging, 31(6), July, pp. 939–946.

[9] Neumann, W., Schad, L. R., and Zllner, F. G., 2017. "A novel 3d-printed mechanical actuator using centrifugal force for magnetic resonance elastography". In 2017 39th Annual International Conference of the IEEE Engineering in Medicine and Biology Society (EMBC), pp. 3541–3544.

[10] Uffmann, K., Abicht, C., Grote, W., Quick, H. H., and Ladd, M. E., 2002. "Design of an MR-compatible piezoelectric actuator for MR elastography". Concepts in Magnetic Resonance, 15(4), Dec., pp. 239–254

[11] Chan, W. C., Sze, K. L., Samartzis, D., Leung, V. Y., and Chan, D., 2011. "Structure and Biology of the Intervertebral Disk in Health and Disease". Orthopedic Clinics of North America, 42(4), Oct., pp. 447–464.

[12] Chen, J., Ni, C., and Zhuang, T., 2006. "Imaging mechanical shear waves induced by piezoelectric ceramics in magnetic resonance elastography". Chinese Science Bulletin, 51(6), Mar., pp. 755–760.

[13] Arani, A., Eskandari, A., Ouyang, P., and Chopra, R., 2017. "A novel high amplitude piezoceramic actuator for applications in magnetic resonance elastography: a compliant mechanical amplifier approach". Smart Materials and Structures, 26(8), p. 087001.

[14] O'Connell, G., Vresilovic, E., and Elliott, D. M., 2009. "Comparative Intervertebral Disc Anatomy Across Seven Animal Species". In 52nd Annual Meeting of the Orthopaedic Research Society.